


Article

# Invariants of Bonded Knotoids and Applications to Protein Folding

Neslihan Gügümcü <sup>1,2,\*</sup>, Bostjan Gabrovsek <sup>3</sup>  and Louis H. Kauffman <sup>4,5</sup>

<sup>1</sup> Department of Mathematics, Izmir Institute of Technology, Gülbahçe Campus, Izmir 35430, Turkey

<sup>2</sup> Mathematics Institute, Georg-August University Göttingen, Bunsenstrasse 3-5, 37073 Göttingen, Germany

<sup>3</sup> Faculty of Mathematics and Physics, University of Ljubljana, 1000 Ljubljana, Slovenia

<sup>4</sup> Department of Mathematics, Statistics and Computer Science, University of Illinois at Chicago, 851 South Morgan St., Chicago, IL 60607-7045, USA

<sup>5</sup> Department of Mechanics and Mathematics, Novosibirsk State University, Novosibirsk 630090, Russia

\* Correspondence: neslihangugumcu@iyte.edu.tr

**Abstract:** In this paper, we study knotoids with extra graphical structure (bonded knotoids) in the settings of rigid vertex and topological vertex graphs. We construct bonded knotoid invariants by applying tangle insertion and unplugging at bonding sites of a bonded knotoid. We demonstrate that our invariants can be used for the analysis of the topological structure of proteins.

**Keywords:** knotoids; proteins; protein folding

## 1. Introduction

A protein consists of a linear chain of amino acids that are linked together by peptide bonds. Pairs of intramolecular sites in a linear chain may be linked with each other with different types of bonds (e.g., disulfide bridges) that yield the folding pattern of the protein, i.e., determine the unique shape of the chain in 3-dimensional space. See Figure 1a.

There is a rising interest of studying protein topology including a subset of its bonds. Progress has been recently made studying the topology of proteins with bonds using the concept of  $\Theta$ -curves (embeddings of the graph in the shape of the Greek letter  $\Theta$  into  $\mathbb{R}^3$ ). The two most notable results were obtained in [1], where they identified seven topologically inequivalent protein  $\Theta$ -curve topologies and in [2], where  $\Theta$ -curve analysis was used to study knots appearing during DNA replication.

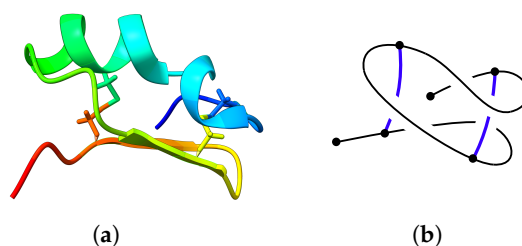


**Figure 1.** The PiTX-K $\beta$  Emperor scorpion toxin with two disulfide bonds (pdb 1c49). (a) A ribbon diagram, (b) Simplified presentation as a bonded knotoid.

The classical knot theory studies knotted and linked loops without free ends. From a knot theory perspective, bonded knotted structures were also studied in [3–5]. Recent works with *knotoids* [6–9] allow us the use of knotted diagrams with free ends, taking the restriction that topological equivalences are not allowed to pass arcs in the diagrams across the free ends.

In our model, we use graphs and embeddings of graphs to represent the molecules, and we model primarily the special bonds that are involved with the protein folding.



**Citation:** Gügümcü, N.; Gabrovsek, B.; Kauffman, L.H. Invariants of Bonded Knotoids and Applications to Protein Folding. *Symmetry* **2022**, *14*, 1724. <https://doi.org/10.3390/sym14081724>

Academic Editors: Erica Flapan and Helen Wong

Received: 30 June 2022

Accepted: 16 August 2022

Published: 18 August 2022

**Publisher's Note:** MDPI stays neutral with regard to jurisdictional claims in published maps and institutional affiliations.



**Copyright:** © 2022 by the authors. Licensee MDPI, Basel, Switzerland. This article is an open access article distributed under the terms and conditions of the Creative Commons Attribution (CC BY) license (<https://creativecommons.org/licenses/by/4.0/>).

We utilize *bonded knotoid diagrams* for our model, which were proposed initially in [4] for topological analysis of open protein chains. A bonded knotoid diagram refers to the graphical structure of the model, where we use some parts of the graph to represent these special bonds. See Figure 1 where we illustrate a partially realistic ribbon diagram of the molecule (left) and then a depiction of the associated bonded knotoid diagram that we take as a topological model for the molecule (right) in which the bonds are illustrated in blue. We base our modeling on topological bonds whose endpoints are trivalent nodes, so that the bond itself is seen as an edge in the graph. We assume that the bond is either *rigid* in the sense that a twisting of one end of the bond is accompanied by a twisting of the other end or *non-rigid* in the sense that a twisting of one end is not necessarily accompanied by a twisting of the other end. In either case, bonded knotoid diagrams are subjected to a collection of topological equivalence moves, and a *bonded knotoid* refers to a class of equivalent diagrams.

In this paper, we construct topological invariants of bonded knotoids by combining a number of methods from knot theory. We use invariants of embedded graphs and generalize knotoids to *graphoids*. We use two methods in this paper called *unplugging* and *tangle insertion* that were initially discussed in [10] to construct invariants for graphoids, specifically for bonded knotoids. The unplugging method removes a node from the related graph by disconnecting an edge that is incident to the node. In tangle insertion, we replace the node by a chosen collection of weaving patterns (*tangles*). We then examine the knotoid or multi-knotoid diagram that arises from the unplugging or tangle insertion and make topological conclusions about the original graphoid. We conclude our paper by demonstrating a concrete application of the bonded knotoid invariants introduced on a specific bonded knotoid diagram representation of the PiTX-K $\beta$  Emperor scorpion toxin with two disulfide bonds, as shown in Figure 1a.

## 2. Preliminaries on Graphoids and Bonded Knotoids

**Definition 1.** A *graphoid* is a spatial graph, that is, a graph embedded in the three-dimensional Euclidean space  $\mathbb{R}^3$ . A graphoid contains exactly two vertices of degree one and a number of vertices whose degrees may vary and are greater than one. The two one-valent vertices of a graphoid are considered to be marked to distinguish them from other vertices. In Figure 2, we illustrate a graphoid with two one-valent vertices marked in red and two vertices of degree four.

There is an infinite collection of pairs of parallel lines passing through the marked one-valent vertices of a graphoid. One can set up a topological equivalence for graphoids by picking up one pair of parallel lines from this collection and considering continuous deformations of graphoids in the ambient space relative to these lines that keep marked vertices on the chosen lines during the deformation. See also Section 3.3 for a discussion on the *rail closure* of graphoids determined by a specific choice of a pair of parallel lines passing through the marked vertices.

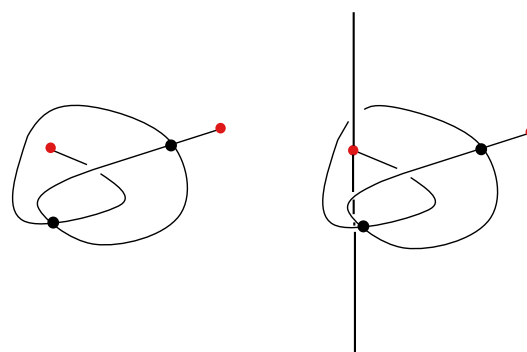


**Figure 2.** A graphoid and two parallel lines through its marked vertices.

**Definition 2.** A graphoid diagram is a representation of a graphoid in a plane that is obtained by projecting the graphoid along a pair of parallel lines passing through its marked one-valent vertices onto the plane the lines are perpendicular to. In a graphoid diagram, edges may intersect at either vertices of degree greater than one that correspond to vertices of the graphoid in  $\mathbb{R}^3$  or interior points of the edges. Each interior intersection is transversal and endowed with over or under information according to the weaving of the graphoid in  $\mathbb{R}^3$ , and it is called a crossing of the graphoid diagram.

A multi-graphoid is a spatial graph with exactly  $2n$  marked vertices of degree one, where  $n \geq 1$ , and a finite number of vertices of any degree.

Two (multi-) graphoid diagrams are considered to be equivalent if they are related to each other by a sequence of Reidemeister moves (R-0, R-I, R-II, R-III) and vertex moves (V-I, V-II), as illustrated in Figure 3. A graphoid in  $\mathbb{R}^2$  refers to a class of equivalent graphoid diagrams. Notice that the vertices that take part in these moves are not marked, and it is not allowed to pull a strand across any of the marked vertices. See Figure 4 for the forbidden moves for the marked vertices shown in red.

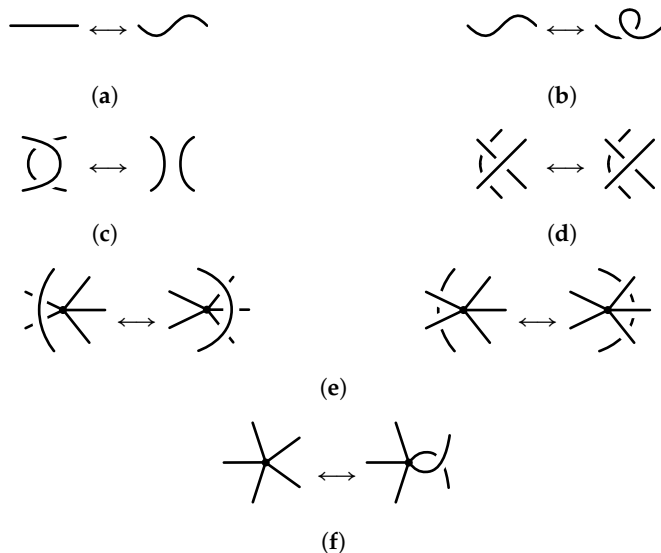


**Figure 3.** Equivalence moves for graphoid diagrams. (a) R-0 (planar isotopy), (b) R-I, (c) R-II, (d) R-III, (e) V-I, (f) V-II.



**Figure 4.** The forbidden moves for marked vertices.

Note that vertices of a graphoid diagram are considered as topological vertices by the allowance of V-II move, that is, one-sided twisting of the edges incident to a vertex. In the sequel, we present bonded knotoid diagrams that contain *bond edges* that are considered to be rigid in the sense that a twist applied at one of the ends of a bond should be applied to the other end of the bond.

**Definition 3 ([9]).** A knotoid diagram is an immersion of the unit interval  $[0, 1] \subset \mathbb{R}$  into the two-dimensional Euclidean space  $\mathbb{R}^2$  with a finite number of crossings that are transversal self-intersections endowed with over or under passage information. The images of 0 and 1 under the immersion map do not coincide with each other and any of the crossings. They are regarded as endpoints of the knotoid diagram and specifically called the tail and the head, respectively. Knotoid diagrams can be considered as graphoid diagrams that contain only two vertices of degree one and one edge connecting these vertices with a number of crossings on it.

A *multi-knotoid diagram* generalizes the notion of a knotoid diagram, containing a number of circle components immersed in  $\mathbb{R}^2$  in addition to one knotoid component.

The equivalence relation on graphoid diagrams restricts to an equivalence relation on knotoid diagrams, which is generated by the Reidemeister moves R-0, R-I, R-II and R-III given in Figure 3.

**Definition 4 ([4]).** A *bonded knotoid diagram* is a pair  $(K, \mathbf{b})$  where  $K$  is a knotoid diagram and  $\mathbf{b}$  is a finite collection of arcs embedded in  $\mathbb{R}^2$ , each of which connects two distinct interior points of  $K$ . The bonds can interact with other edges of the diagram or each other, as illustrated in Figure 5.

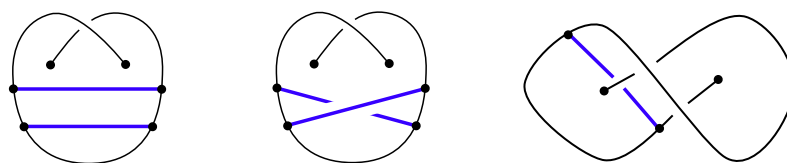


Figure 5. Examples of bonded knotoid diagrams where bonds are shown in blue.

We consider the bonds as edges, each connecting two trivalent vertices so that the pair  $(K, \mathbf{b})$  can be viewed as a special graphoid diagram where the bond edges are distinguished from other edges. Bond edges of a bonded knotoid diagram can be considered as either *rigid* or *non-rigid*. By rigidity of a bond, it is meant that a 180 degree rotation of a bond results in twisting both sides of the bond (see the first move in Figure 6), while non-rigidity assumption allows one-sided twisting under the rotation of the bond (see Figure 7). The equivalence relation we consider on bonded knotoid diagrams depends on the assumption on the type of bonds.

Two bonded knotoid diagrams with rigid bonds are considered to be *equivalent* if they can be transformed to each other by a sequence of Reidemeister moves and *bond moves* of type I, II, and III, as shown in Figure 6.

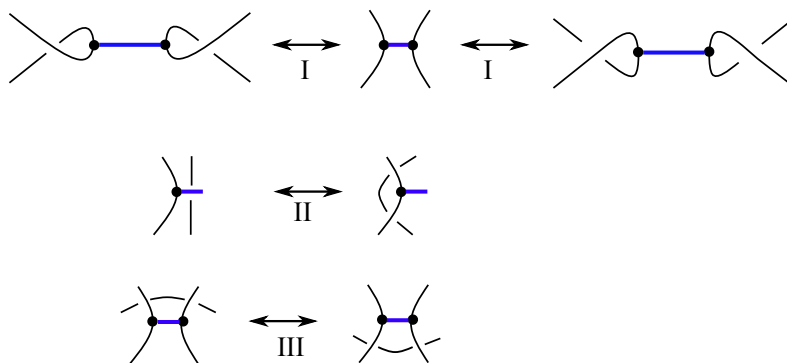


Figure 6. Bond moves.

In the non-rigid approach, two bonded knotoid diagrams are assumed to be *equivalent* if they are related to each other by sequence of Reidemeister moves, bonded moves of type II and III and also the non-rigid bond move of type I that allows one-sided twisting of a bond under a 180-degree rotation in the plane. The non-rigid type I move is shown in Figure 7.

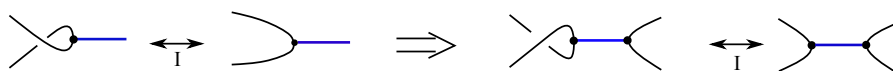


Figure 7. A non-rigid bond move of type I.

### 3. Topological Invariants of Bonded Knotoids

#### 3.1. Invariants Induced by Tangle Insertion

In [4,5,11], it is discussed that the folding of a bonded molecular structure such as a protein backbone with bonds or RNA can be modeled by a bonded knotoid diagram (or a bonded knot diagram through a viable closure) and detected by bonded knotoid invariants induced by *tangle insertions* at bonding sites. A *tangle insertion* is to replace a *bonding site* of a bonded knotoid diagram (or a bonded knot diagram) that consists of only a bond with its adjacent vertices, considered as rigid, with specific choices of tangles to obtain a multi-knotoid diagram (or a link diagram in the case of a bonded knot diagram). The bonding site at which that the tangle insertion is applied is required not to interact with itself or other edges of the bonded knotoid diagram except at the adjacent vertices to the bond edge in the site.

**Definition 5.** A *contracted bond* of a bonded knotoid diagram is a straight edge with two distinct trivalent vertices incident to it and without any interactions with itself or other strands of the diagram.

It is not hard to see that any bonded knotoid diagram can be transformed to a bonded knotoid diagram containing only contracted bonds. The transformations can be realized by pushing the bond vertices through intersecting strands via a sequence of bonded moves II and III. In Figure 8, we illustrate a transformation of a bond into a contracted bond.

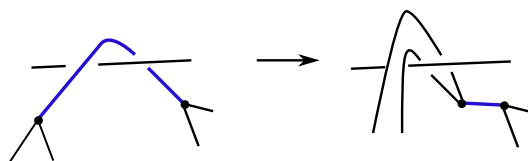


**Figure 8.** A bond transforms into a contracted bond via equivalence moves.

One can determine the tangle types to be utilized in tangle insertion according to the equivalence relation assumed for rigid bonded knotoid diagrams (Figure 9). Figure 10 shows that a rigid bonded type II move demands the inserted tangle to be isotopic to its horizontal reflection. A *rational tangle* is a tangle that can be constructed by starting with two horizontal or two vertical strands, picking two endpoints and twisting them, then picking another pair and twisting them, and so on, for a finite number of twists [12,13]. Rational tangles are a good choice for tangle insertions since they are invariant under 180 degrees of vertical or horizontal rotation in the plane [12]. With choices of rational tangles to be inserted in bonding sites, an equivalence between any two bonded knotoid diagram induces an equivalence between multi-knotoid diagrams resulting from the tangle insertion at the bonding sites of the bonded knotoid diagrams. This fact implies that a choice of tangle insertion into the nodes of a rigid vertex graph will give invariants of the graph from any invariants of the links obtained by the insertion.

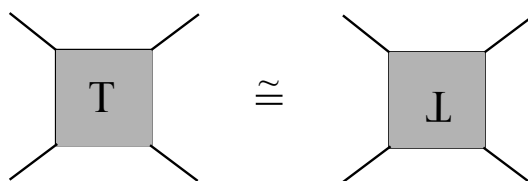


**Figure 9.** Tangle insertion under horizontal reflection.

We utilize the Kauffman bracket expansion [14] at the bonding sites to have the *double twist bracket polynomial*. We do this first by inserting the *empty tangle*, the *right-handed full twist tangle* and the *left-handed full twist tangle* at the bonding sites, where the inserted tangles are considered to be parallel to the neighboring strands of the bond. We then calculate the

formal linear sum of the Kauffman bracket polynomials of the resulting knotoid diagrams, with formal coefficients  $a, b, c$ .

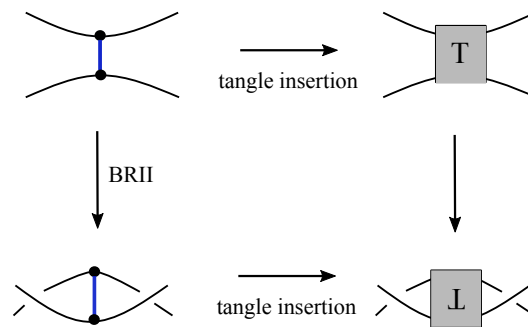


Figure 10. Tangle inserted at a bonding site is chosen to be isotopic to its horizontal reflection.

As we verify in Figure 11, one crossing knotoid diagram with only one bond is non-trivial topologically, as its double twist bracket polynomial is non-trivial.

$$\begin{aligned}
 \langle \text{Diagram 1} \rangle &= a \langle \text{Diagram 2} \rangle + b \langle \text{Diagram 3} \rangle + c \langle \text{Diagram 4} \rangle \\
 \langle \text{Diagram 5} \rangle &= a \langle \text{Diagram 6} \rangle + b \langle \text{Diagram 7} \rangle + c \langle \text{Diagram 8} \rangle \\
 &= -a A^{-3} - b A^{-9} - c A^3
 \end{aligned}$$

Figure 11. Bracket expansion at a bonding site.

**Proposition 1.** *The double twist bracket polynomial is a regular isotopy invariant of bonded (multi-)knotoids. That is, the double twist bracket polynomial is invariant under Reidemeister moves of type II and III but not of type I move.*

**Proof.** In Figure 12, we show the invariance under a rigid bond move of type II. The invariance under the other moves can be shown in a similar fashion. Adding a small curl to a bonded knotoid diagram by a type I Reidemeister move multiplies the double twist bracket polynomial of the diagram by  $-A^3$  if the curl is right-handed and  $-A^{-3}$  if the curl is left-handed. See Figure 13 for an illustration.  $\square$

$$\begin{aligned}
 \langle \text{Diagram 1} \rangle &= a \langle \text{Diagram 2} \rangle + b \langle \text{Diagram 3} \rangle + c \langle \text{Diagram 4} \rangle \\
 &= a \langle \text{Diagram 5} \rangle + b \langle \text{Diagram 6} \rangle + c \langle \text{Diagram 7} \rangle \\
 &= \langle \text{Diagram 8} \rangle
 \end{aligned}$$

Figure 12. Invariance under a bonded move of type II.

$$\langle \text{Diagram 1} \rangle = A \langle \text{Diagram 2} \rangle + A^{-1} \langle \text{Diagram 3} \rangle = -A^3 \langle \text{Diagram 4} \rangle$$

$$\langle \text{Diagram 5} \rangle = A \langle \text{Diagram 6} \rangle + A^{-1} \langle \text{Diagram 7} \rangle = -A^{-3} \langle \text{Diagram 8} \rangle$$

**Figure 13.** The bracket is not invariant under R-I moves.

Note that one can choose any rational tangle collection to be inserted at the bonding sites for the bracket expansion. In this way, we obtain an infinite collection of brackets induced by each choice of tangle insertion. None of the induced bracket polynomials is invariant under a R-I move, and this means that molecules that differ in writhe may have different invariants. One can *normalize* a bracket polynomial as in [14] to compensate for the writhe and induce a polynomial that is invariant under R-I, R-II and R-III moves.

**Definition 6.** The normalized double twist polynomial of an oriented (multi-)knotoid diagram  $K$ ,  $f_K$  is given as follows.

$$f_K(A, A^{-1}) = (-A^3)^{-w(K)} \langle K \rangle,$$

where  $w(K)$  is the *writhe* of  $K$ , which is obtained by summing up the signs of crossings of  $K$ .

#### Oriented Case

A knotoid diagram admits a natural orientation from one of its endpoints to the other one: conventionally from its tail to its head. The orientation on a bonded knotoid diagram induces two different types of oriented bonding sites, an *anti-parallel bonding site*, where the orientation arrows on the local strands neighboring a bonded site are directed oppositely, and a *parallel bonding site*, where the orientation arrows on the local strands neighboring a bonded site point to the same direction; see Figure 14. Oriented bonded knotoid diagrams can be utilized to analyze open protein backbones that admit a natural orientation from one end (N-terminus) to the other end (C-terminus). Tangle insertion can be applied directly for oriented bonding sites by specific choices of rational tangles, and one can utilize knotoid invariants on the resulting oriented multi-knotoid diagram such as the arrow polynomial [4,7] and the affine index polynomial [7,15].



**Figure 14.** An anti-parallel site and a parallel bonding site.

In [4,16], bonds of an oriented knot and knotoid diagram are interpreted as *rigid vertices* that are graphical vertices admitting a determined cyclic order of its incident edges. This interpretation is provided by contracting an anti-parallel bonding site to a disoriented rigid vertex and a parallel bonding site to an *oriented rigid vertex* with respect to the orientation on its incident edges. Then, to utilize topological invariants of knots or knotoids, each rigid vertex is replaced with certain rational tangles. We note here that our interpretation of bonds of oriented bonded knotoid diagrams coincides with the rigid vertex interpretation of bonds of an oriented bonded knotoid diagrams with a fixed collection of tangles to be used for tangle insertion; see Figure 15. However, for unoriented bonded knotoid diagrams, the bond–rigid vertex correspondence is not one-to-one anymore, since vertical and horizontal bonds both are contracted to the same rigid vertex.

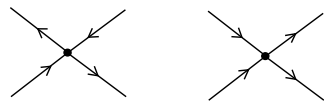


Figure 15. Disoriented and oriented rigid vertices.

### 3.2. Invariants Induced By Unplugging

The unplugging invariant  $T$  of spatial graphs was introduced in [10], and in [17], the invariant was extended to edge-colored spatial graphs. In this section, we extend this invariant to graphoids, edge-colored graphoids, and rail graphs. As a special case, it can be used to distinguish non-rigid bonded knotoids.

The unplugging invariant  $T$  for graphoids is constructed as follows. At each vertex of a graphoid  $G$ , we make a *local replacement* as depicted in Figure 16; for a vertex of degree  $n > 1$ , there are  $\frac{n(n-1)}{2}$  choices for a replacement. Note that the newly formed free ends are unmarked.

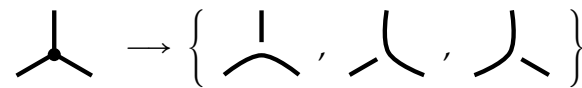


Figure 16. A local replacement at a vertex.

Let  $r(G)$  denote the multi-knotoid diagram formed by performing local replacements for each vertex, where we also remove all unknotted arcs, except if this arc contains both endpoints (marked vertices). We denote by  $T(G)$  the collection of multi-knotoids for all possible replacements  $r(G)$ .

**Theorem 1.** *The set  $T(G)$ , whose elements are taken up to their multi-knotoid type, is an invariant of  $G$ .*

**Proof.** The collection  $T(G)$  is invariant under the Reidemeister moves, which is, as in the classical case [10], easy to check.  $\square$

Given two graphoids,  $G_1$  and  $G_2$ , the sets  $T(G_1)$  and  $T(G_2)$  can be compared by any invariant of multi-knotoids, e.g., the Kauffman bracket polynomial or the Kauffman bracket skein module [3].

As an example, we compute the unplugging invariants for bonded knotoid diagrams  $A$  and  $B$  given in Figure 17, which differ from each other by a bond swap. In [3], it is shown that the Homflypt skein module of bonded links does not detect bond swaps; however, the unplugging invariants show that  $A$  and  $B$  are indeed different.

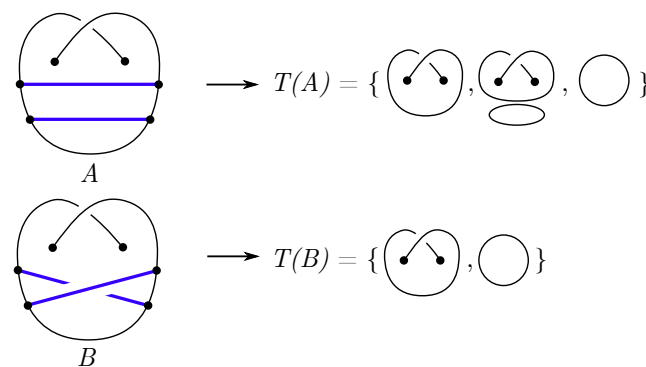


Figure 17. Two bonded knotoids and their unplugging invariant.

We can also consider *colored graphoids*, i.e., a graphoid diagram  $G$  together with a coloring function

$$c : E(G) \rightarrow C,$$



where  $E(G)$  is the set of edges of  $G$  and  $C$  is a set of colors; we will extend the unplugging invariant  $T$  to a colored version, denoted by  $T_{\text{col}}$  (see also [17] for a similar construction for generalized  $\Theta$ -curves).

Let  $a, b$ , and  $c$  be the colors of the edges incident to  $v$ . We define a colored local replacement as a local replacement, where, in addition, we color each new arc by  $\gamma \subset \{a, b, c\}$ , where  $\gamma$  contains the colors of the preimage of the replacement according to the image in Figure 18.

Similarly as before,  $r_{\text{col}}(G)$  denotes the colored multi-knotoid diagram formed by performing local replacements for each vertex, where we also remove all unknotted arcs, except if this arc contains both marked endpoints. We denote by  $T_{\text{col}}(G)$  the collection of multi-knotoids for all possible colored replacements  $r_{\text{col}}(G)$ .

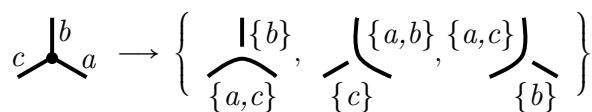


Figure 18. A colored local replacements at a vertex.

**Theorem 2.** *The set  $T_{\text{col}}$ , whose elements are taken up to their multi-knotoid type, is an invariant of colored graphoids.*

**Proof.** Again, invariance under Reidemeister moves is easy to check; see [10,17].  $\square$

We can take the set of colors  $C = \{0, 1\}$  and color the edges belonging to a non-rigid bonded knotoid diagram by 0 and the edges, belonging to the bonds, by 1. See Section 4 for an example. Naturally, we can expand the coloring set if we want to distinguish different types of bonds.

### 3.3. Invariants Induced by Unpluggings of the Rail Closure

We associate to a bonded knotoid diagram  $B$  a long graphoid diagram  $R(B)$ , called the rail closure of  $B$ , by the following procedure: At each marked endpoint of  $B$ , we draw a vertical line in the plane in such a way that the upper segment, starting from the endpoint, goes above the rest of the diagram, and the segment below the endpoint goes below the rest of the diagram, as depicted in Figure 19 [18]. The long graphoid diagram  $R(B)$  corresponds to the diagram of the graphoid embedded in three-dimensional space  $\mathbb{R}^3$  that is obtained by adding lines, perpendicular to the plane of  $B$ , through each of the marked endpoints of  $B$ .

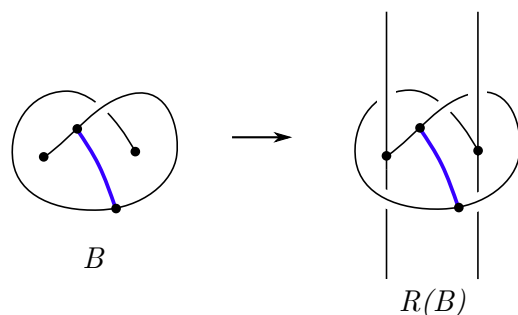


Figure 19. A bonded knotoid diagram  $B$  and its rail closure.

Note that the equivalence between non-rigid bonded knotoid diagrams extends to the equivalence between rail closures, i.e.,  $B_1 \cong B_2 \Leftrightarrow R(B_1) \cong R(B_2)$ . The unplugging invariant  $T$  is also well defined in the setting of rail closures, the resulting collection  $T(R(B))$  of a bonded knotoid diagram  $B$  is a set of long knots with possible multiple long arcs.

We conclude this section by giving some applications of rail closures.

In the first example, we consider the two knotoid diagrams  $k$  and  $k^*$  in Figure 20. The two non-trivial unpluggings (local replacements)  $T$  and  $T^*$  of the rail closures  $R(k)$  and

$R(k^*)$ , respectively, represent mirror images of the long trefoil knot. Since the trefoil knot is chiral, we can conclude that  $k$  and  $k^*$  are not equivalent.

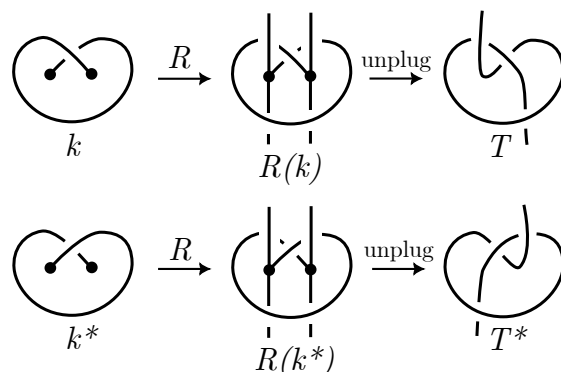


**Figure 20.** Two knotoids (left), their rail closure (middle) and their local replacements (right). Since  $T \not\cong T^*$ , it follows  $k \not\cong k^*$ .

In the second example, we demonstrate a verification that the bonded knotoid diagram  $G$  given in Figure 21 is not equivalent to the trivial bonded knotoid  $H$ . If we take the rail closure of  $G$  and perform a tangle insertion on one of the unpluggings by the horizontal empty tangle, we obtain a long link with linking number  $\pm 1$ , which we could not obtain if  $G$  was equivalent to the trivial bonded knotoid diagram  $H$ . It follows that  $G \not\cong H$ .

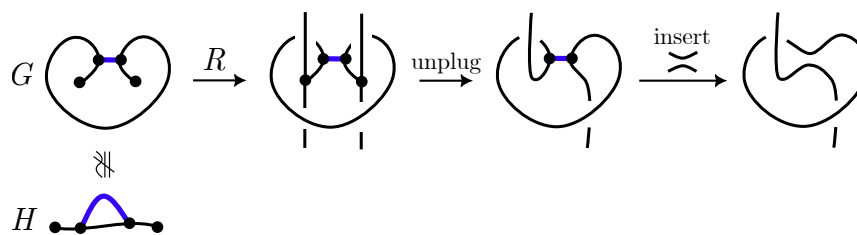


**Figure 21.** The bonded knotoid  $G$  is not equivalent to the trivial bonded knotoid  $H$ .

In the third example (Figure 22), we show that the unplugging invariant of the rails of knotoids  $k$  and  $k^*$  fails to detect they are not equivalent (see [19], where it is shown that the parity bracket detects  $k \not\cong k^*$ ). In the four-crossing unpluggings of the rail closures of the knotoids, we obtain the long figure eight knots  $E$  and  $E^*$ . Since the figure eight knot is not chiral, we cannot conclude  $k \not\cong k^*$ . However, if we consider bonded knotoids  $l$  and  $l^*$ , which correspond to knotoids  $k$  and  $k^*$  after adding a bond (Figure 23), perform a tangle insertion and consider the five-crossing unpluggings of the rail closures, we obtain two long chiral three-twist knots,  $K$  and  $K^*$ , which are mirror images of each other. We can conclude  $l \not\cong l^*$ .

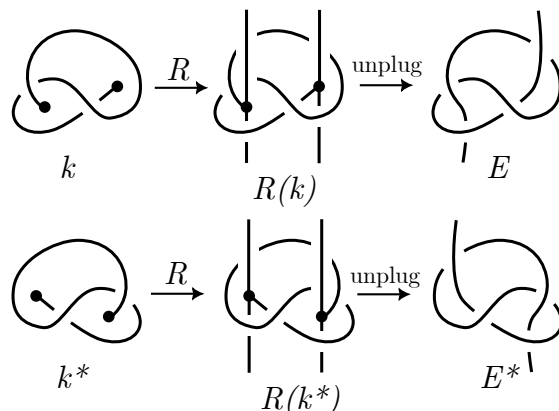


**Figure 22.** The unplugging invariant on the rail closures does not distinguish  $k$  and  $k^*$ .

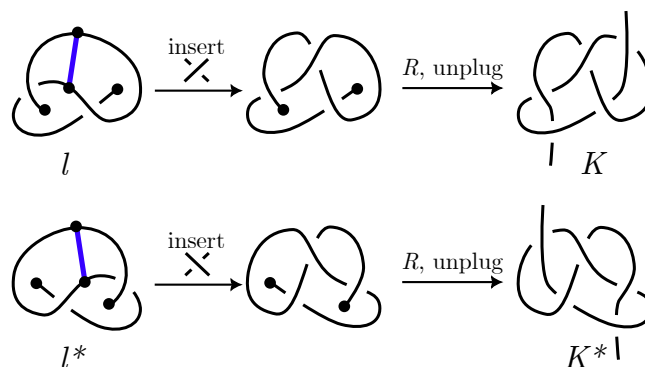


**Figure 23.** The unplugging invariant on the rail closures of  $l$  and  $l^*$ , after a tangle insertion, shows  $l \neq l^*$ .

**4. An Application**

In Figure 1a, we view the ribbon diagram of the protein PiTX-K $\beta$  with two disulfide bonds and the corresponding bonded knotoid diagram. We denote the corresponding bonded knotoid diagram by  $K$ , which is shown also in Figure 24.

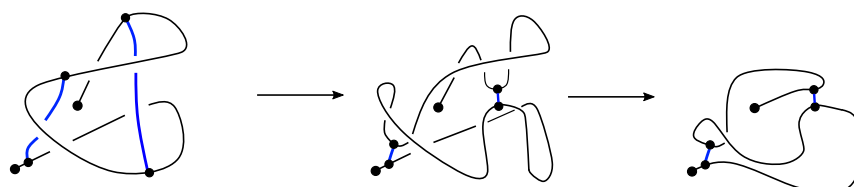


**Figure 24.** An equivalence transformation between bonded knotoid diagrams  $K, K',$  and  $K''$ .

We first model the two disulfide bonds to correspond to rigid bonds in the bonded knotoid diagram  $K$ . To be able to apply tangle insertion, each bond of  $K$  is transformed to a contracted bond by bonded moves of type II and III so that we obtain the bonded knotoid diagram  $K'$  illustrated in the middle of Figure 24. We simplify  $K'$  by deleting curls by a sequence of three R-I moves for the ease of calculation to obtain the final diagram in Figure 24. Let us denote the simplified bonded knotoid diagram by  $K''$ .

In Figure 25, we illustrate all multi-knotoid diagrams that are obtained by tangle insertions at the bonding sites of  $K''$ , with the corresponding commuting formal coefficients. By routine calculation, it can be verified that the double twist bracket polynomial of  $K''$ ,  $\langle K'' \rangle = -a^2 A^{-3} + ab (-A^{-1} - A^{-3} + A^{-7} + A^6) + bc (A^8 - A^4 + 2 - A^{-4} + A^{-8}) + b^2 (A^8 - A^4 - A^{-4} + A^{-2} - A^{-6} + 2) + ca (A^{-6} - A^{-5} - A^{-3} + A) + c^2 (A^{-8} - A^4 - A^{-4} + A^2 - A^6 + 2)$ .

It is not hard to verify the following equality.

$$\langle K' \rangle = -A^{-3} \langle K'' \rangle .$$

By using the equality above, one can easily compute the double twist polynomial of  $\langle K' \rangle$  that is assigned to the protein PiTX-K $\beta$ .

For the unplugging invariant (Figure 26), we color the strand representing the backbone by 0 and the disulfide bonds by 1. A direct computation, using the colored local replacement rule presented in Figure 18, gives the following collection of multi-knotoid types.

With this example, we have illustrated the process of applying our work to actual molecules or to partially realistic models of molecules. One makes the appropriate choices and observations on the representation of the molecule to replace it with a bonded knotoid graph. Then, the topological analysis of this graph can proceed, and we can understand in this way the limitations of the form of the molecule imposed by topological structure. We hope that molecular biology researchers will see in this paper a wide array of ideas that can be used in practical applications of protein and RNA analysis.

$$\begin{aligned}
 \langle \text{Knot} \rangle &= a^2 \langle \text{Diagram 1} \rangle + ab (\langle \text{Diagram 2} \rangle + \langle \text{Diagram 3} \rangle) \\
 &+ bc (\langle \text{Diagram 4} \rangle + \langle \text{Diagram 5} \rangle) + b^2 \langle \text{Diagram 6} \rangle \\
 &+ ca (\langle \text{Diagram 7} \rangle + \langle \text{Diagram 8} \rangle) + c^2 \langle \text{Diagram 9} \rangle
 \end{aligned}$$

Figure 25. Calculating the double twist bracket polynomial.

$$\text{Knot} \xrightarrow{\text{unplug}} \left\{ \left[ \begin{array}{c} \bullet \\ | \\ \bullet \end{array} \right], \left[ \begin{array}{c} \bullet \\ | \\ \bullet \\ | \\ \bullet \end{array} \right], \bigcirc \right\}$$

Figure 26. Calculating the unplugging invariant.

**Author Contributions:** Conceptualization, N.G., B.G. and L.H.K.; methodology, N.G., B.G. and L.H.K.; software, N.G., B.G. and L.H.K.; validation, N.G., B.G. and L.H.K.; formal analysis, N.G., B.G. and L.H.K.; writing—review and editing, N.G., B.G. and L.H.K. All authors have read and agreed to the published version of the manuscript.

**Funding:** The first author’s research was supported by the Dorothea Schlözer Postdoctoral Program by Georg-August University, Göttingen. The second author’s research was supported by the Slovenian Research Agency program P1-0292.

**Institutional Review Board Statement:** Not applicable.

**Informed Consent Statement:** Not applicable.

**Data Availability Statement:** Not applicable.

**Conflicts of Interest:** The authors declare no conflict of interest.

## References

- Dabrowski-Tumanski, P.; Goundaroulis, D.; Stasiak, A.; Sulkowska, J.I.  $\theta$ -curves in proteins. *arXiv* **2019**, arXiv:1908.05919.
- O’Donnol, D.; Stasiak, A.; Buck, D. Two convergent pathways of DNA knotting in replicating DNA molecules as revealed by  $\Theta$ -curve analysis. *Nucleic Acids Res.* **2018**, *46*, 9181–9188. [[CrossRef](#)] [[PubMed](#)]
- Gabrovšek, B. An invariant for colored bonded knots. *Stud. Appl. Math.* **2021**, *146*, 586–604. [[CrossRef](#)]
- Goundaroulis, D.; Gügümcü, N.; Lambropoulou, S.; Dorier, J.; Stasiak, A.; Kauffman, L. Topological models for open-knotted protein chains using the concepts of knotoids and bonded knotoids. *Polymers* **2017**, *9*, 444. [[CrossRef](#)]
- Kauffman, L.H.; Magarshak, Y.B. *Vassiliev Knot Invariants and the Structure of RNA Folding*; Series on Knots and Everything Knots and Applications; World Scientific: Singapore, 1995; pp. 343–394.
- Diamantis, I. Knotoids, pseudo knotoids, braidoids and pseudo braidoids on the torus. *arXiv* **2021**, arXiv:2103.16433.
- Gügümcü, N.; Kauffman, L.H. New invariants of knotoids. *Eur. J. Comb.* **2017**, *65*, 186–229. [[CrossRef](#)]
- Goundaroulis, D.; Dorier, J.; Benedetti, F.; Stasiak, A. Studies of global and local entanglements of individual protein chains using the concept of knotoids. *Sci. Rep.* **2017**, *7*, 6309. [[CrossRef](#)] [[PubMed](#)]
- Turaev, V. Knotoids. *Osaka J. Math.* **2012**, *49*, 195–223.
- Kauffman, L.H. Invariants of graphs in three-space. *Trans. Am. Math. Soc.* **1989**, *311*, 697. [[CrossRef](#)]
- Tian, W.; Kauffman, L.H.; Liang, J. A knot polynomial invariant for analysis of topology of RNA stems and Protein disulfide bonds. *Comput. Math. Biophys.* **2017**, *5*, 21–30. [[CrossRef](#)] [[PubMed](#)]
- Goldman, J.R.; Kauffman, L.H. Rational tangles. *Adv. Appl. Math.* **1997**, *18*, 300–332. [[CrossRef](#)]
- Kauffman, L.H.; Lambropoulou, S. On the classification of rational tangles. *Adv. Appl. Math.* **2004**, *33*, 199–237. [[CrossRef](#)]
- Kauffman, L.H. *New Invariants in the Theory of Knots*; Société Mathématique de France Astérisque: Marseille, France, 1988; p. 137.
- Kauffman, L.H. An affine index polynomial invariant of virtual knots. *J. Knot Theory Ramif.* **2013**, *22*, 1340007. [[CrossRef](#)]

16. Kauffman, L.H. Knot diagrammatics. In *Handbook of Knot Theory*; Elsevier Science: Amsterdam, The Netherlands, 2005; pp. 233–318.
17. Gabrovšek, B.; Gügümcü, N. Invariants of multi-knotoids. *arXiv* **2022**, arXiv:2204.11234.
18. Kodokostas, D.; Lambropoulou, S. Rail knotoids. *J. Knot Theory Ramif.* **2019**, *28*, 1940019. [[CrossRef](#)]
19. Gügümcü, N.; Kauffman, L.H. Parity, virtual closure and minimality of knotoids. *J. Knot Theory Ramif.* **2021**, *30*, 2150076. [[CrossRef](#)]